ADVANCED MATERIALS TECHNOLOGIES
www.advmattechnol.de

# A Soft-Rigid Gripper for Safe Handling and Transportation

*Danilo Troisi,* Mihai Dragusanu, Maria Pozzi, Domenico Prattichizzo, and Monica Malvezzi*

**The automatic handling of perishable items like food and agricultural products requires robotic grippers that not only can perform gentle grasps but can also transport grasped objects safely and reliably. This result can be obtained by assuring that the contact between the grasped object and the gripper is as extended as possible, to avoid stress concentration in small areas, that could lead to local damage. In this study, a soft-rigid gripper is presented and designed to grasp and hold objects and to distribute the contact pressure over a large surface, limiting its maximum value and avoiding localized peaks. The gripper has four fingers and an extendable soft palm that wraps around the object, resembling a soft pocket. The palm is composed of two soft parts, whose geometrical characteristics have been evaluated using a shape optimization process and can be easily detached from the fingers to be changed or washed. The gripper is characterized with mechanical tests and evaluated in grasping and transporting tasks with real objects.**

## 1. Introduction

Robotic manipulation of perishable items has applications in different domains, from food industry[1] to agriculture,[2] up to household assistance.[3] According to a recent review, handling food items with robotic manipulators poses three main challenges:[4] *i)* design of suitable end-effectors, *ii)* food recognition, and *iii)* estimation of food products' properties (e.g., size, shape, weight, softness, fragility, and ease of bruising).

The first aspect deals with the problem of developing grippers that can grasp objects with different physical properties and adhere to hygienic and operation requirements related to the food handling application (including bio-compatible materials, easy-to-wash structures, gentle grasp, fast transportation, low power consumption, contamination, and bruising avoidance). Several robotic grippers have been designed with these features in mind in the last few years.[5] However, finding the right trade-off between system robustness, efficiency, and adaptability to different tasks, with a reasonably contained amount of actuators and sensors is still an open challenge, especially when dealing with deformable or uncertain shape objects.[6]

In this paper, we propose a soft-rigid gripper specifically thought for grasping and transporting perishable foods, like fruits and vegetables. The gripper is composed of four soft-rigid passive fingertips mounted on an actuated soft-rigid palm. The former allows the gripper to gently approach and grasp objects, whereas the latter is designed for safe transportation (**Figure 1**). With the term *safe* in this paper we refer to object preservation: the gripper can maintain a reliable grasp in the presence of dynamic effects (e.g. abrupt accelerations, impacts with the surrounding environment, etc.), without applying high localized pressure that could damage it. The design of the soft part was achieved through a shape optimization process. This process included setting precise constraints to redistribute stresses across the petal structure, aiming to minimize displacement of the grasped object within the gripper. Rather than designing the internal part as a continuum soft bag, the structure is composed of multiple petal-shaped elements and provides an efficient trade-off between the enveloping capabilities of smaller objects and the possibility of grasping larger, non-spherical objects. The proposed gripper is actuated by only one motor, that activates the mechanism opening-closure movement. The compliance of the inner part provides adaptability to different object shapes, dimensions, and characteristics. The mechanism allowing the gripper to open and close, and the peculiar petal geometrical shape, make the gripper efficient from an energy consumption point of view. In addition, since the motor is placed in the base of the gripper, the parts that enter in contact with grasped objects can easily be detached and washed/exchanged. The paper is organized as follows. After a brief summary of related works on soft-rigid grippers for food handling (Section 2), the methodology adopted to design the gripper is explained (Section 3). The results of the gripper characterization and testing are then presented and discussed in

D. Troisi, M. Dragusanu, M. Pozzi, D. Prattichizzo, M. Malvezzi
Department of Information Engineering and Mathematics
University of Siena
Via Roma, 56, Siena 53100, Italy
E-mail: troisi@diism.unisi.it
D. Troisi
Department of Information Engineering
University of Pisa
Via Girolamo Caruso, 16, Pisa 56122, Italy
M. Pozzi, D. Prattichizzo
Istituto Italiano di Tecnologia
Via Morego, 30, Genova 16163, Italy

The ORCID identification number(s) for the author(s) of this article can be found under https://doi.org/10.1002/admt.202401592



**DOI: 10.1002/admt.202401592**

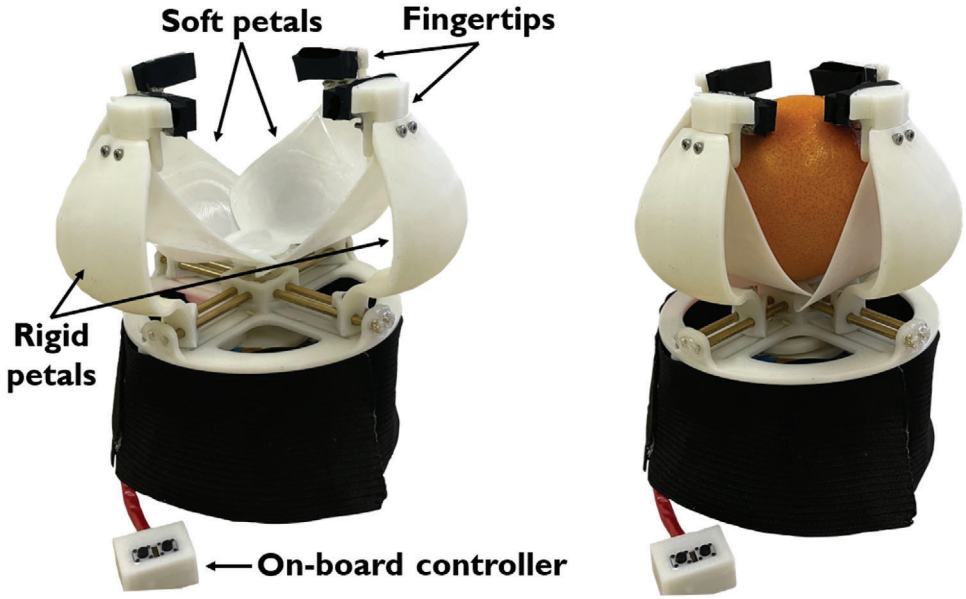


**Figure 1.** Prototype of the gripper. It has a soft-rigid actuated palm for safe transportation and four soft-rigid fingertips for delicate grasping.

Section 4 and 5, respectively. Conclusion and future work are outlined in Section 6.

## 2. Related Works

Grasping and transporting perishable items like food and agricultural products requires robotic grippers with specific design features.[4,7] One of the main requirements is that of preventing the damage of grasped objects. Multiple solutions to this problem have been proposed in literature, from embedding tactile sensors in the fingertips to accurately control contact forces,[8] to building soft end-effectors that distribute forces over the object by maximizing the contact area.[9,10] Recently, He et al.[11] proposed a combination of these two principles, by developing soft pneumatic sensorized fingertips for grasping small delicate objects. Wang et al.[12] and Jain et al.,[13] instead, introduced a multimodal gripper capable of precise gentle grasps through structures placed at the fingertips (suction cups, nails), and of enveloping grasps using pneumatic fingers. In Ref. [14], Piskarev et al. proposed a dual-technology gripper combining granular jamming and electroadhesion to address limitations in handling flat, fragile, or oily surfaces, achieving superior performance in complex grasp-and-release tasks. Similarly,[15] introduced a thermo-actuated, aphid-inspired adhesive gripper that employs 3D-printed Polylactic Acid (PLA) with shape-memory properties. These innovations underline the necessity for integrative approaches, as exemplified by our soft-rigid gripper, which focuses on safe and gentle handling of perishable food items through its modular and hygienic design. Recent advances in multimaterial 3D printing process made possible the development of grippers that combine variable stiffness and embedded sensing capabilities. In 2023, Goh et al.[16] introduced a 3D-printed artificially innervated smart soft gripper capable of tuning its stiffness on-demand through Joule heating. This gripper integrates conductive PLA to adjust the rigidity and soft Thermoplastic polyurethane (TPU) into a monolithic structure. Such integration represents a promising direction in delicate object handling (Supporting Information).

In this paper, we do not embed specific sensors in the gripper to keep its structure as light and simple as possible, and we embrace the idea of using soft adaptable structures to wrap objects and handle them safely. However, we do not adopt a fully soft structure, but rather combine soft and rigid materials. Soft-rigid grippers have the advantages of compliant devices (e.g., intrinsic safety and adaptability[17–19]), but still allow complex tasks like handling of deformable objects,[20] in-hand manipulation,[21,22] and environmental constraints exploitation.[23]

In the literature, some examples of bio-inspired robotic grippers where the enveloping structures have a petal-like structure have been recently introduced. Jain et al.[13] present a compact design of soft actuators and passive compliant mechanisms able to reconfigure the gripper to perform different tasks. Zhang et al.[24] propose a bio-inspired gripper with petals constituted by bistable composites, pneumatically controlled. Wang [25] analyses shape–morphing robotic structures and exploits them in petal-like components. A flat, flower-shaped gripper applying an electrostatic adhesive to grasped objects is presented by Schaler et al.[26]

Differently from Refs. [13, 24], the gripper developed in this paper employs an electric servomotor to move rigid parts that consequently drag the attached soft parts. This allows keeping the electronics of the control and power supply systems directly inside the base of the gripper, without the encumbrance of wires or tubes going from the gripper to external sources, as would happen in pneumatic actuation. While the petals in Ref. [24] have a bistable behavior, and then a finite set of configurations is allowed, in this work the gripper closure can be continuously controlled within the workspace. Compared with the solution proposed in Ref. [13], where multiple actuators are combined for specific grasping tasks, the gripper proposed in this paper employs an actuator only and its adaptability to different object shapes is

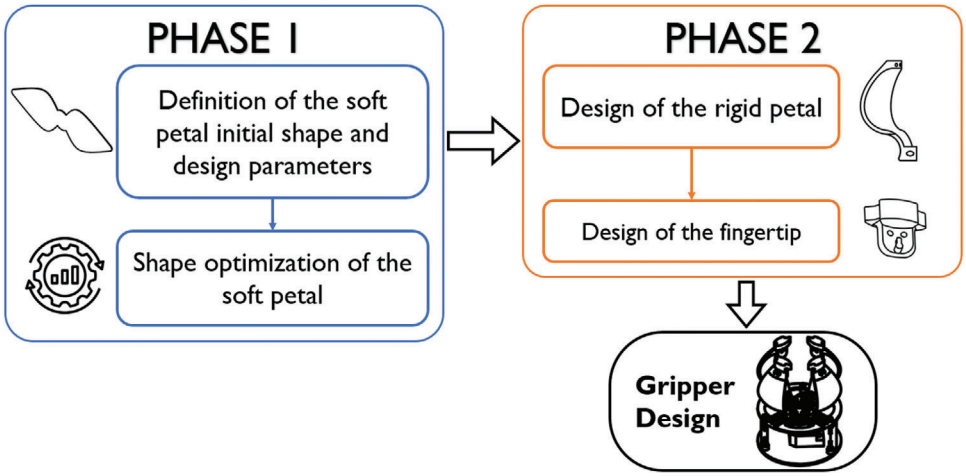


**Figure 2.** Procedure adopted for the gripper structure design.

provided by its internal compliant structure. The petals of the gripper proposed in this paper are manufactured with standard FDM (Fused Deposition Modeling) processes, employing plastic materials (TPU for the soft parts, Acrilonitrile Butadiene Stirene (ABS) or PLA for the rigid ones), differently from,[24,26] where specific manufacturing technologies and materials are employed. Our choice is motivated by the envisaged gripper applications (e.g. agriculture and food handling), which often require cleaning, disinfection, and maintenance operations that would be difficult with such types of sophisticated structures and materials.

The rigid and soft petals parts of the gripper form an actuated palm that envelops objects after they are grasped by the fingertips. In robotic grippers, palm actuation is still not a prominent feature but usually adds important functions,[27] from thumb opposition,[28] to novel grasping and manipulation abilities.[29,30] Similarly to Refs. [31, 32], but with different mechanisms, palm actuation allows to envelop the object and to vary the size of the gripper workspace.

In classical grasping tasks involving rigid and approximately undeformable objects, grasp properties are evaluated by means of well-established, geometry-based structural properties depending on contact point location and contact friction properties.[33] Even when the gripper is underactuated, the main aspects that are considered in grasping evaluation are grasp robustness with respect to uncertainties in the applied load[34] also referred to as grasp resilience.[35] Dealing with perishable items like fruits or agricultural products, requires considerations about how contact pressure patterns localized in small patches of the object could produce damage on it.[36,37] In the gripper proposed in this paper, this aspect has been taken into account by developing a soft structure that hosts the object once it is grasped, enveloping it and avoiding excessive local pressure peaks.

## 3. Methodology

The developed gripper is underactuated and uses a soft-rigid palm to grasp/release and safely transport objects like food items, fruits and vegetables. The prototype is shown in Figure 1 and is composed of an actuated palm made of soft and rigid petals, and soft-rigid fingertips.

The methodology used to design the gripper can be divided into two main phases, which are summarized in **Figure 2** and are described in the following subsections. A detailed overview of the gripper design is reported at the end of the section.

### 3.1. Phase 1: Design of the Soft Petals

The objective of the first phase is to design and optimize the soft part of the palm, i.e., the soft petals. The design starts from a symmetrical structure consisting of two opposite petals and their connection in the center of the palm; by combining one, two, or more of these structures, different types of grippers can be obtained. The design of the soft petals can be further divided into two main steps (Figure 2): *i)* definition of the initial shape and design parameters, and *ii)* shape optimization.

The dimensions of the petals were initially determined by considering the typical size and shape of commonly handled fruits, vegetables and food items. Moreover, the shape of the petals is motivated by the idea of having a soft structure able to envelop the grasped object assuring a wide contact surface. The petals are then further developed by performing a shape optimization with the aim of minimizing object movement during transportation.

The initial parametric CAD model of the two petals with defined profiles joined together at the base is shown in **Figure 3a**. The structure is flat and the main parameters for each petal are the length $L_{petal}$ and the maximum width $W_{petal}$, whereas the parameter common to the two petals is the diameter $Ø_{petal}$ of the circumference joining them and the thickness $th_{petal}$, see Figure 3a. The parameters are initially set to: $L_{petal} = 85$ mm, $W_{petal} = 57$ mm, $Ø_{petal} = 28$ mm and $th_{petal} = 1$ mm.

The shape optimization is aimed at minimizing the displacement of the petal when it is subject to external loads simulating the presence of an object. The optimization problem was defined using the Structural Mechanics module of COMSOL Multiphysics 6.0, in which the petal is defined using the Shell interface.[38] The material used for the simulations is Flex-45 thermoplastic co-polyurethane (Young modulus: $E = 94$ MPa, Poisson's ratio: $\nu = 0.4$) and the shell thickness is 1 mm. Polyurethane was selected because of its fatigue resistance and elongation,

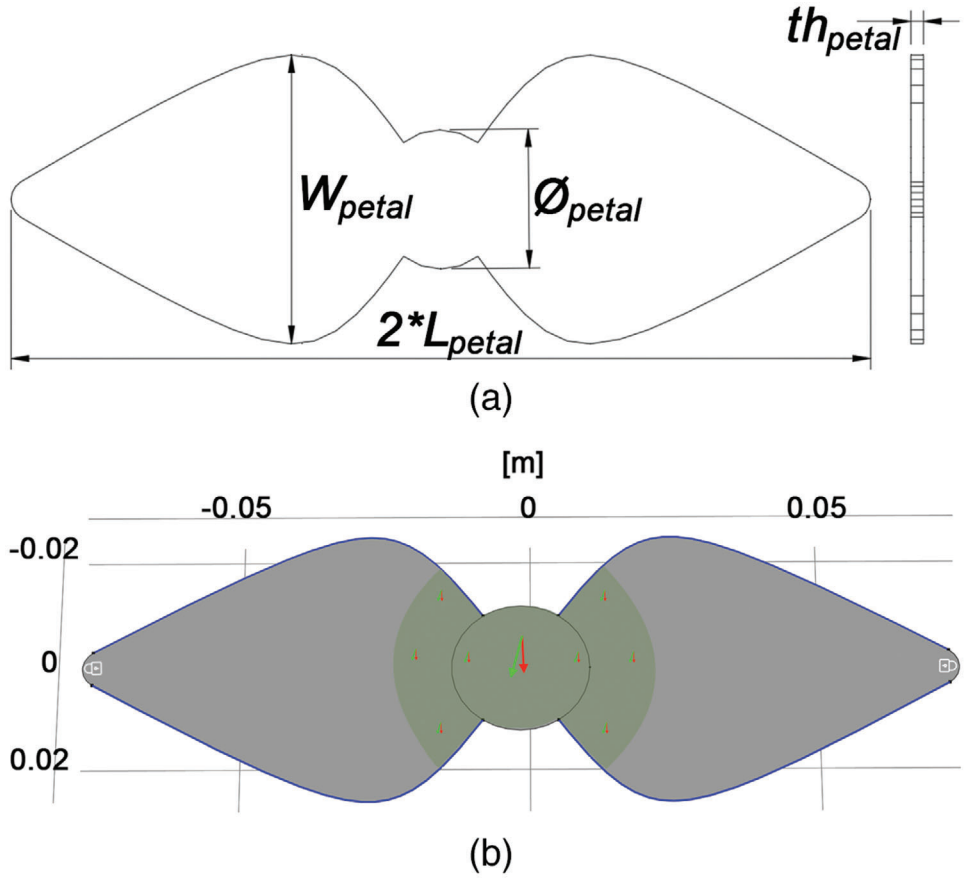


**Figure 3.** Initial soft petal design: a) Technical drawing of the model with shape parameters, b) model imported in COMSOL simulator with applied forces and constraints.

which allow repeated movements of the gripper without damaging the structure, and because it is able to provide a good damping ratio suitable for reducing undesired vibrations.[39] Polyurethane is also non-toxic, non-marking, non-allergenic, and resistant to mineral and vegetable oils and aromatic hydrocarbons, so it is widely adopted in food-grade applications.

To simulate the operative conditions in which the petals are inserted into the gripper and fixed to the rigid petals (Figure 1), the external edges are constrained. This is indicated with a white padlock symbol in Figure 3b. To simulate the presence of an object, normal and tangential forces are applied in the central area of the petals, shown in green in Figure 3b. The applied normal and tangential forces are depicted through red and green arrows, respectively. The lateral edges (in blue in Figure 3b) are fixed to preserve the initial predetermined petal profile after the optimization. The simulator is thus constrained to modify only the internal structure domain and the center where the two petals are rigidly joined together. The shape optimization was conducted for different combinations of normal and tangential force values. The normal force was bounded to vary between 1 and 10 N, whereas the tangential varied between −10 and 10 N. We chose these values to take into account different possible weights of the grasped objects, considering typical weights of fruit and vegetables with sizes compatible with that of the envisaged petals.

Initial simulations of the petal with uniform thickness subject to a force in the central part with both normal and tangential components, both 1 N, reported maximum values for the equivalent Von Mises stress of about 4.5 MPa and a maximum displacement magnitude of 6.5 mm. The shape optimization results are shown in **Figure 4**. The petal parameters in terms of maximum length and width are $L_{petal}$ = 84.75 mm and $W_{petal}$ = 56.9 mm, respectively. It can be noticed that the shape optimization outputs a new structure of the petals with the same shape but a variable thickness, resulting in a concave surface in the central part of the petal, while the circular part joining the two petals has an approximately elliptic shape with the semi-axes 14.86 and 13.22 mm, respectively. The scale adopted in Figure 4 goes from 0, where no changes to the initial shape occurred, to 1, where the most relevant changes occurred.

To verify the improvements obtained after shape optimization, a structural analysis was conducted, in which a force with both tangential and normal components equal to 1 N, is applied. Results in terms of equivalent Von Mises stress and displacement magnitude are shown in **Figure 5**. In this loading condition, the maximum displacement, in the central part of the petal, is equal to 3.46 mm, and the maximum equivalent Von Mises stress is 3.14 MPa, as shown in Figure 5.

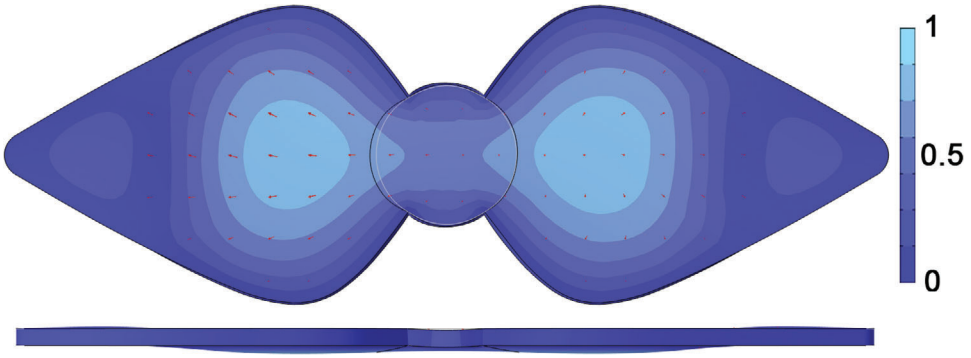


**Figure 4.** Results of the shape optimization, top and lateral view with the relative scale: 0 means that there is no change in shape while 1 indicates the regions in which the shape change the most.

### 3.2. Phase 2: Design of the Rigid Part

The rigid part of the gripper structure consists of a petal-shaped rigid support and an interchangeable fingertip module, which is covered by a rubber layer added to increase fingertip friction and to guarantee safe grasp operation. The fingertip is designed also to allow the connection of the soft petals. The shape of the rigid part of the gripper is designed in a parametric way, in particular, it can be adapted to the length and width of the optimized petal. Moreover, this support allows the petals to wrap the object once it is grasped thanks to the internal support space designed to house the soft petals while they adapt to the object. This part of the

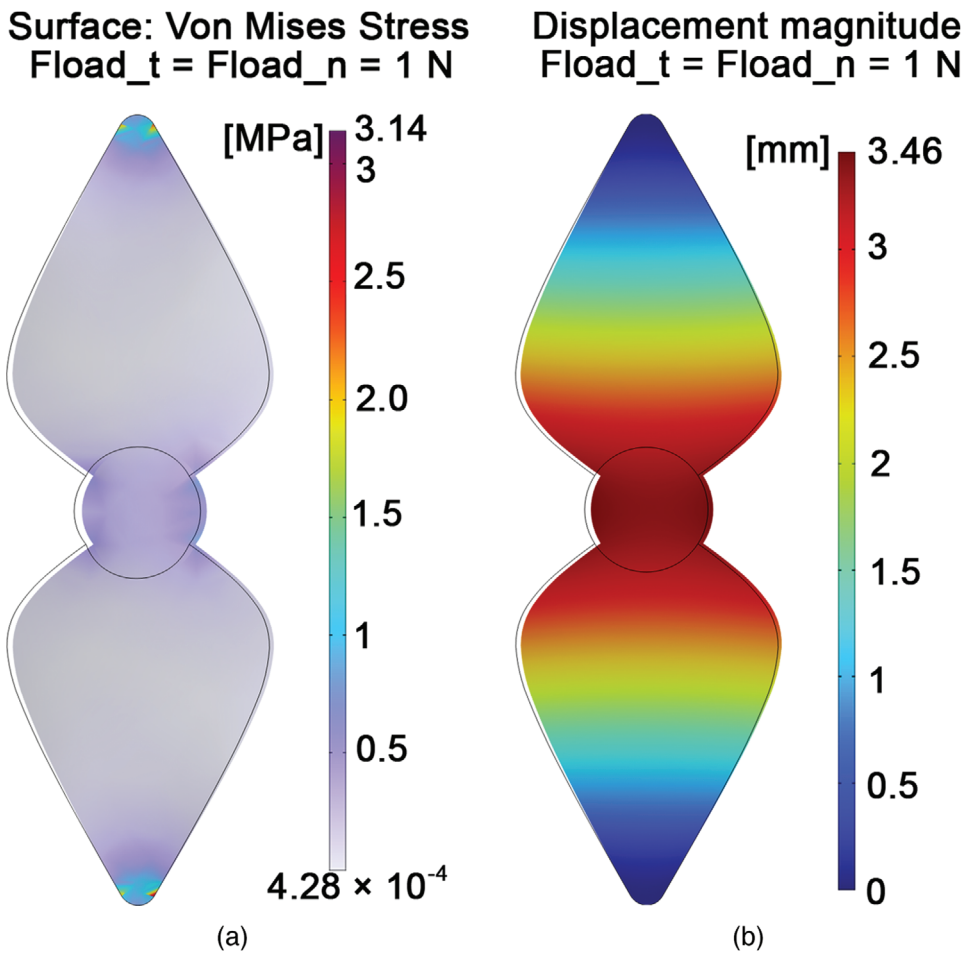


**Figure 5.** Optimized soft petal design: results of the structural analysis in terms of a) stress distribution, and b) total displacement. The grey contour is the initial position of the petals before the application of forces.

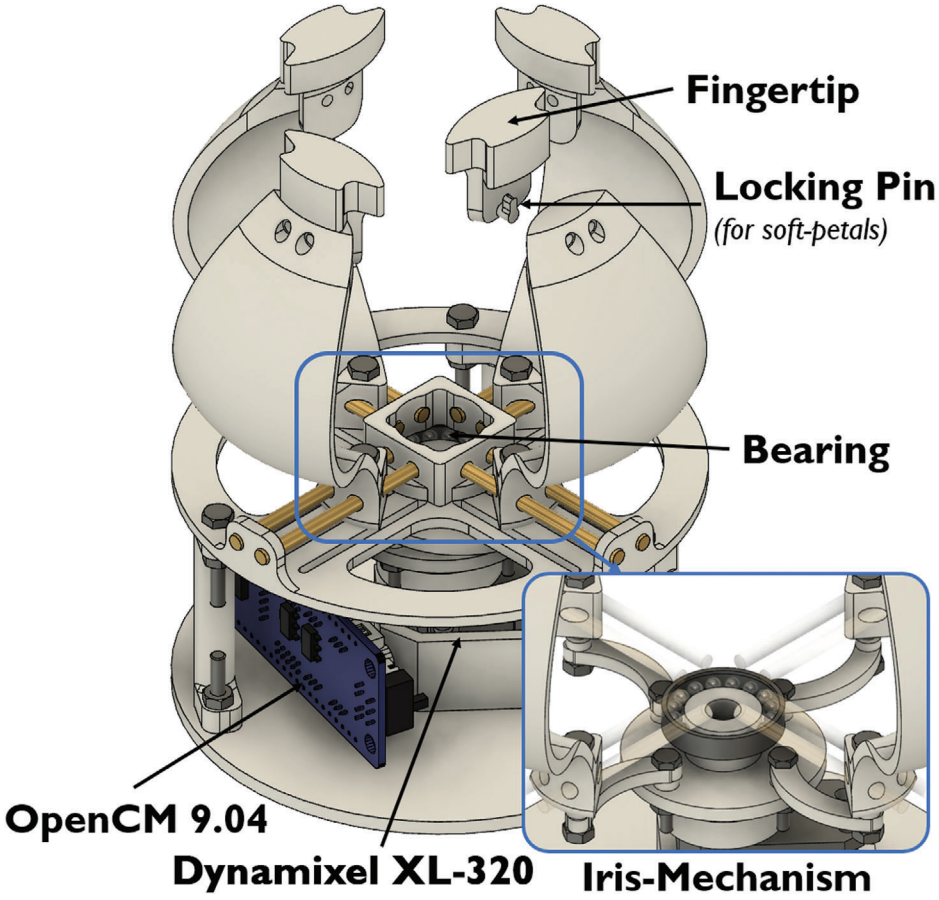


**Figure 6.** CAD model of the gripper.

gripper has to be stiff enough to provide a reliable support for the soft internal part and to resist the object weight and possible external collisions, preventing the object to be bruised. At the same time, it has to be easy to manufacture and as light as possible, to limit the overall weight of the gripper. For these reasons the chosen material is ABS.

### 3.3. The Gripper Structure

In this subsection, we provide details on the design of the gripper structure, whose CAD model is shown in **Figure 6**. As previously introduced, the gripper presents a soft internal part capable of enveloping objects. The soft part is supported by a rigid part, which is composed by fingertips attached to external rigid petals which resemble the soft internal ones. These latter elements are connected to an actuated base providing the opening/closure movement and containing all the electronic components.

The gripper has only one motor, which allows to actuate all the four rigid support petals through an Iris mechanism. For the application presented in this work, a Dynamixel XL-320 is employed, having a maximum torque of 0.39 Nm and a maximum angular speed of 11.93 rad $s^{-1}$. This actuator presents several features that are useful in the envisaged application, including low voltage, simple control, good position feedback and very small size that allows the gripper to be light, compact, and easy to handle.

The four external petals are arranged in a symmetrical configuration and move together during opening and closing. By applying a rotation to the shaft that is connected to the motor, the Iris mechanism allows to obtain four translational motions, since the petals are constrained in their guides, as shown in Figure 6. Furthermore, to improve the overall gripper robustness and guarantee a precise motion, we chose to use two brass bars for each petal that work as additional guides, supporting the petal structure and constraining the rotation of the petals with respect to their symmetry axis. Between the shaft and the plate that hosts the guides, a bearing allows to reduce the friction during opening-closing. Attached to each petal there is an interchangeable fingertip covered by a rubber layer made in ethylene-vinyl acetate foam, which is fixed on the rigid petal thanks to two small screws. Moreover, as shown in Figure 6, on the back side of the fingertip, there is a pin on which an extremity of the soft petal is fixed. The actuation of the gripper modifies the volume inscribed within the rigid petals, which will host the grasped object enveloped by the soft petals. Since the fingertips are not actuated, the actuation system also defines their configuration. Depending on the mechanical transmission characteristics and on the rigid petal shape, the overall fingertip stroke can be evaluated, which also defines the minimum and maximum dimensions of the objects that can be

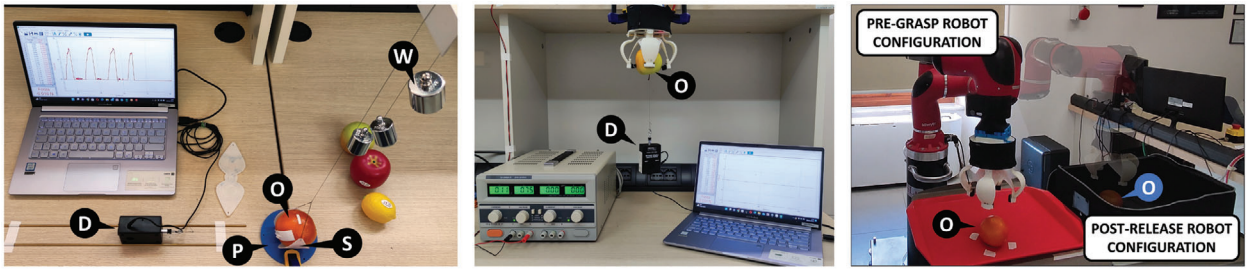


(a) Experiment 1 (b) Experiment 2 (c) Experiment 3, 4

**Figure 7.** Experimental setups for: a) characterizing the soft petals, b) evaluating the maximum grasp strength of the gripper, c) testing the gripper grasping abilities. Legend: (D) – Dynamometer; (O) – Tested object; (P) – Support plate for soft petals; (S) – Soft petals under testing; (W) – Weights.

grasped. More details on the features of the gripper are reported in **Table 1**.

For gripper control, an OpenCM 9.04 microcontroller (Robotis, South Korea) is used, with the Dynamixel driver and an ARM Cortex-M microcontroller. The gripper is powered with two Li–Po batteries of 3.7 V each and for this application a simple position control with changeable proportional gain is implemented. The opening-closing motion can be achieved both via serial USB or via Bluetooth communication through a RN-42 Bluetooth module (Roving Networks Inc., United States). This system guarantees a transmission range up to 20 m, and it requires very low energy consumption (Absorbed Current: 26 A in sleep-mode, 30 mA in transmition-mode; Input Voltage: 3.3 V DC). A wired remote to directly command the gripper by pressing two buttons was also installed (Figure 1). All electronic components and the motor are placed in the gripper base, in a safe position and well-protected from accidental contacts and shocks.

Regarding employed materials, all the rigid parts are made of ABS, whereas the soft petals are made of Flex-45 thermoplastic. The total weight of the gripper is 228 g, the fingertip stroke is 19.2 mm, the maximum diameter is 158 mm, and the height is 138 mm. The geometric characteristics define the workspace of the gripper which can be adapted based on the set of objects that need to be grasped.

## 4. Experimental Section

The gripper was tested with four experiments: the first aimed at characterizing the soft petals obtained through the optimization procedure described in Section 3; the second aimed at evaluating the maximum grasp strength of the gripper; the third aimed at testing the gripper grasping abilities; the fourth aimed at testing the gripper capability of holding an object at different levels robot velocities. The adopted experimental setups are shown in **Figure 7**, whereas the used objects are listed in **Table 2**. As we target the manipulation of food items, we chose a set of real and plastic fruits and vegetables with different properties (shape, weight, texture). The plastic ones belong to the YCB Dataset[40] and were included because they have different sizes and weights and present surfaces with very low roughness.

**Table 1.** Main specifications of the gripper.

| Item | Specifications |
|---|---|
| Type of gripper | Servo-Electric |
| Degrees of Actuation | 1 |
| Weight | 227.63 [g] |
| Size ($Ø_{closed}$ ~ $Ø_{open}$) x H | (115 ~ 158) [mm] x 138 [mm] |
| Fingertips stroke | 19.2 [mm] |
| Materials | ABS, Flex-45 thermoplastic co-polyurethane, brass |
| Microcontroller | ROBOTIS OpenCM 9.04 |
| Communication | USB, Bluetooth, Wired remote |

### 4.1. Experiment 1: Characterization of the Soft Petals

To have insights on their actual performance, in this experiment, three different versions of the soft petals were selected and tested. The experiment aimed at evaluating the soft petals' capability of wrapping objects and holding them when shear forces are applied. For this purpose, a subset of the objects depicted in Table 2

**Table 2.** Properties of the objects used in the experiments. For the size we either specify the length, width and height for cuboid objects, or the maximum diameter and the height for cylindrical ones.

| ID | Object | Weight [g] | Size [mm] |
|---|---|---|---|
| 1 | Lemon (YCB) | 29 | 54 × 68 |
| 2 | Lime | 67.2 | 45 × 50 |
| 3 | Kiwi | 84.5 | 50 × 65 |
| 4 | Apple (YCB) | 68 | 62 × 75 |
| 5 | Apple | 146.7 | 60 × 70 |
| 6 | Orange | 158.7 | 60 × 68 |
| 7 | Avocado | 288.3 | 70 × 115 |
| 8 | Pear | 154 | 68 × 70 |
| 9 | Banana (YCB) | 66 | 36 × 190 |
| 10 | Zucchini | 216 | 34 × 127 |
| 11 | Tangerine | 85 | 45 × 58 |
| 12 | Potato | 125 | 50 × 40 |
| 13 | Apple chips | 26 | 150 × 140 × 20 |
| 14 | Biscuits | 56 | 150 × 90 × 25 |
| 15 | Crackers | 34 | 110 × 50 × 20 |

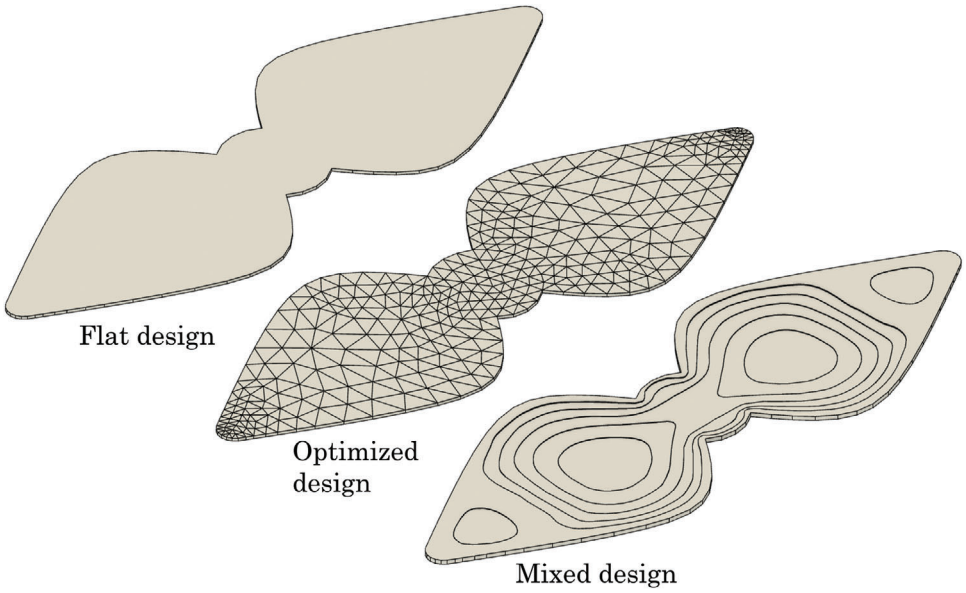


**Figure 8.** CAD of the tested soft petals: flat, optimal, mixed. The flat design is the initial version of the soft petals, the optimized design is the output of the shape optimization, the mixed design is a combination of the first two.

was used. The objects were chosen to assess the response of each pair of soft petals to different shapes, textures, dimensions, and weights.

The three tested pairs of soft petals are depicted in **Figure 8** and are the flat one, which corresponds to the initial design of the soft petals, the optimized one, which is the output of the shape optimization, and the mixed one, which is a combination of the first two soft petals, i.e. the top part is concave while the bottom part is flat.

The soft petals are made using a FlashForge Creator Pro 3D-Printer. The material used for 3D-printing is the Flex-45 thermoplastic co-polyurethane for the soft part, while for the supports we used ABS plastic.

Since the optimized pair of soft petals was not so easily printable due to its convexity that required ABS supports in the 3D-printing phase, we also printed a mixed pair of soft petals having the upper part of the optimized soft petals and the lower part of the flat soft petals.

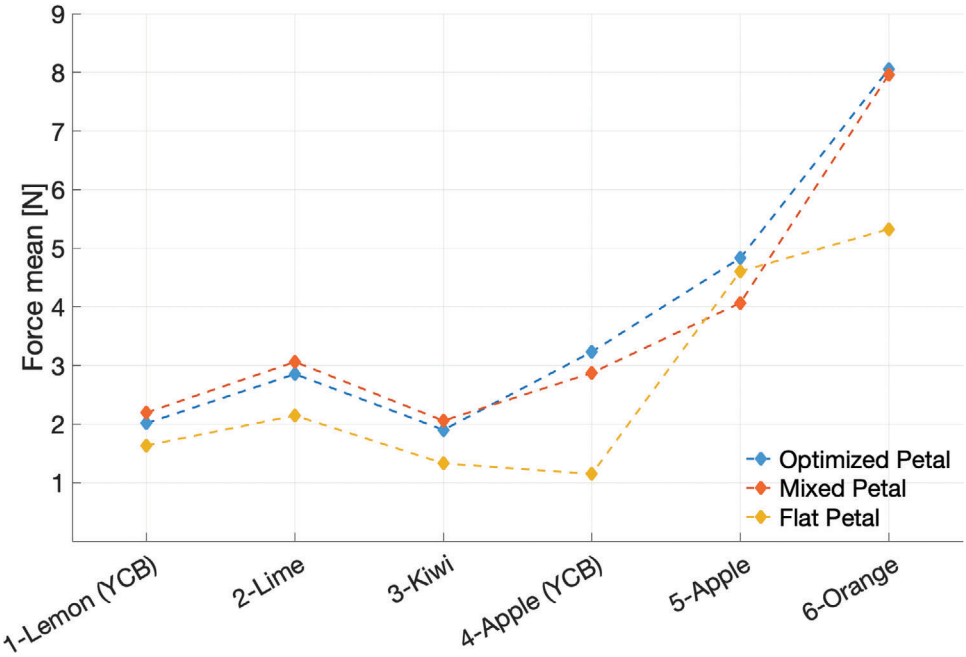


**Figure 9.** Results of Experiment 1: average peak force value at which the slippage occurred for different objects. The mixed pair of soft petals performs similarly to the optimal one.

To obtain these new petals, the areas of the different regions of the optimized soft petals (shown in Figure 4 with different colors) were projected onto a flat surface and extruded based on the values of the scale in Figure 4. The scale indicates the entity of changes applied to the different regions of the structure with respect to the initial non-optimized part, going from 0 (no change) to 1 (highest change). The idea is to transform these values in terms of layer thickness, associating 0 to the maximum thickness for that region and 1 to the minimum thickness value. The latter is computed as the maximum thickness divided by the number of visible regions having different colors. In the current implementation, the maximum thickness is equal to 1 mm and the number of visible regions is 6, thus the minimum thickness is equal to 1/6 mm. In this way, we obtained a new pair of soft petals that is very similar to the shape-optimized one but is much easier to create through 3D-printing, since it adheres totally to the 3D-printer bed.

The experimental setup of Experiment 1 is shown in Figure 7a. It consists of a digital dual-range Vernier dynamometer (Vernier Software & Technology, United States), labeled as D, with an accuracy of 0.05 N, which is pulled horizontally by an experimenter. The dynamometer is connected to the tested object (O) through a tendon, whereas the pair of soft petals under testing (S) is wrapped around the object by pulling its extremities with a force of 4 N applied vertically through weights (W), while keeping the central part rigidly fixed to a plate (P). In each experimental trial, the dynamometer was pulled until the object slipped away from the petals enveloping it. The peak force value at which the slippage occurred was recorded and averaged over 10 trials per object. Obtained results for the different objects and the different petals are shown in **Figure 9**. The data were acquired with a frequency of 100 Hz.

It is worth noticing how both concave pairs of soft petals respond much better than the flat one for almost all objects. Since the performance of the mixed soft petal was comparable to that of the optimized soft petal, the former was chosen for conducting the subsequent experiments, due to its ease of prototyping.

### 4.2. Experiment 2: Evaluation of the Grasp Strength

To evaluate the gripper strength, we conducted an experiment to determine the maximum vertical force that can be applied to the object without making it slip from the gripper.

During the tests, the gripper was firmly fixed to a surface (see Figure 7b) and four different objects of varying weights, sizes, and textures, were grasped with the fingertips. The same dynamometer used in Experiment 1 was connected to the object through a tendon and was pulled until the object slipped out of the gripper. The force required to break the grasp was recorded four times per object at 100 Hz. Since the gripper was placed in a vertical position, we added the weight force of the object to the average maximum recorded force for each object. The results of the experiment are reported in the third column of **Table 3**.

It is worth noticing that the gripper can hold an object even without power. This is due to the fact that the mechanism at the base of the gripper is hardly back-drivable. This is an advantage in terms of energy consumption and safe transportation of objects. We conducted additional experimental trials like the ones described above to test the gripper grasp strength when the power is switched off and the gripper is performing a power (enveloping) grasp. Results are reported in the fourth column of Table 3.

**Table 3.** Experiment 2 results: grasp strength in fingertip grasp with power on, and in power grasp with power off.

| ID | Object | Fingertip Grasp [N] | Power Grasp [N] |
|---|---|---|---|
| 1 | Lemon (YCB) | 2.98 | 7.84 |
| 4 | Apple (YCB) | 3.94 | 12.38 |
| 5 | Apple | 4.52 | 17.42 |
| 6 | Orange | 3.69 | 16.79 |
| | Average | 3.78 | 13.60 |

### 4.3. Experiment 3: Grasping

This experiment aimed at verifying the grasping and transportation capabilities of the gripper. The device, equipped with the mixed soft petals, was attached to a seven degrees of freedom collaborative robot arm, the Sawyer (Rethink Robotics Inc.), and it was tested with all the objects listed in Table 2. The experimental setup is shown in Figure 7c. Five grasping trials per object were performed. Each trial was divided into four phases, which are: grasp, up-down test, left-right test, and release. While during the grasp and release phases the joint velocities were set to be the 10% of their maximum velocity values, during the test phases they were set to be the 30%.

*Grasp* – the object was placed in a fixed position over a table in front of the robot (see Figure 7c), the robot was controlled in joints position to reach the object and the gripper was closed over the object. Once the grasp was achieved, the object was lifted up in such a way that the gripper palm faced up. In that configuration the gripper was opened and closed again to let the object go from the fingertips to the soft petals. Then, the gripper was put again with the palm facing down following the same trajectory of the first motion, but in the opposite direction.

*Up-Down Test* – The last two joints of the robot were rotated with four steps of $\pi/4$ rad, upwards and downwards. After each step, the robot stopped for 0.5 s. After this, the robot performed the same rotation movements but without stopping in the middle.

*Left-Right Test* – Once the *Up-Down Test* was passed, the object was transported laterally, from left to right, with a motion determined by the rotation of the joint at the basis of the robot of an overall angle of $\pi/4$ rad with steps of $\pi/16$ rad, back and forth, with stops of 0.5 s between each step. The same motion was then repeated in a continuous way without stopping.

*Release* – Lastly, if all the tests were completed successfully, the object was transported to its final position, i.e., in the black box shown in Figure 7c, and released. The results of Experiment 3 are in **Table 4** (**Figure 10**).

### 4.4. Experiment 4

The experimental setup for Experiment 4 was the same as for Experiment 3, and the robot motion was divided in the same

**Table 4.** Results of Experiment 3: grasping and transportation.

| ID | Object | Fail Grasp | Fail U-D Test | Fail L-R Test | Fail Release | Success rate |
|---|---|---|---|---|---|---|
| 1 | Lemon (YCB) | 1/5 | 0 | 0 | 0 | 4/5 |
| 2 | Lime | 2/5 | 0 | 0 | 0 | 3/5 |
| 3 | Kiwi | 2/5 | 0 | 0 | 0 | 3/5 |
| 4 | Apple (YCB) | 0 | 0 | 0 | 0 | 5/5 |
| 5 | Apple | 1/5 | 0 | 0 | 0 | 4/5 |
| 6 | Orange | 0 | 0 | 0 | 0 | 5/5 |
| 7 | Avocado | 0 | 0 | 0 | 0 | 5/5 |
| 8 | Pear | 1/5 | 0 | 0 | 0 | 4/5 |
| 9 | Banana (YCB) | 0 | 0 | 1/5 | 1/5 | 3/5 |
| 10 | Zucchini | 0 | 0 | 0 | 1/5 | 4/5 |
| 11 | Tangerine | 1/5 | 0 | 0 | 0 | 4/5 |
| 12 | Potato | 0 | 0 | 0 | 0 | 5/5 |
| 13 | Apple chips | 0 | 0 | 0 | 2/5 | 3/5 |
| 14 | Biscuits | 0 | 0 | 0 | 1/5 | 4/5 |
| 15 | Crackers | 0 | 0 | 0 | 1/5 | 3/5 |
| | TOTAL | 8/75 | 0 | 1/75 | 6/75 | 60/75 |

four phases. This time, however, we only considered 2 objects, one almost spherical (potato) and one elongated and box-shaped (crackers), handled at four different joint velocities during the test phases: 35%, 40%, 45%, 50% of the maximum joint velocity values. For each velocity level, we performed three trials for each object. As reported in **Table** 5, all the conducted trials were successful in all the phases.

## 5. Discussion

The conducted experiments allowed to characterize different aspects of the developed gripper. We started by testing the grasping capabilities of soft petals evaluating their resistance to lateral pulling forces (Experiment 1, Figure 9). In terms of pulling (tangential) force, it was found that the optimized pair of soft petals and the mixed pair of soft petals can withstand up to 2.5 N more than the flat one when pulling larger objects (ID: 4, 6), and about 1 N more when pulling smaller objects (ID: 1, 2, 3). On average, the flat pair of petals could resist forces up to 2.70 N, whereas the optimized and the mixed pair of petals could resist forces up to 3.81 and 3.70 N, respectively. Only for the apple, the flat pair of petals slightly outperformed the mixed ones, probably because in general the apple has a shape that fits well within the petals, and thus all of them performed similarly. From these results we can observe how the shape optimization played a fundamental role in the correct design of the soft petals, since they can wrap the objects correctly, keeping them from slipping much more than the non-optimized ones. Since the wrapping capability of the mixed pair of petals is comparable with that of the optimized one but is much easier to 3D-print, we adopted it in the subsequent experiments.

Experiment 2 was performed to evaluate the strength of the grasp when a vertical pulling force is applied to the object. When a grasp is executed with the fingertips, the average pulling force that can be resisted considering objects with different weights and textures is 3.78 N. This value could be increased using a more powerful motor, but still allows to grasp several different objects. In addition, the idea is that, during the gripper operation, the fingertip grasp is performed only at the beginning of the grasping task. Then the gripper is rotated with the palm up so that the object falls thanks to the gravity in the soft pocket and gets enveloped by the soft petals.

Eventually, we evaluated the gripper payload in power grasps performed without power supply, when the object is enveloped in the inner part by the soft petals. In this case, the resisted force is 13.60 N on average. This result is particularly interesting as it shows that thanks to its mechanical structure the gripper can withstand large forces without consuming energy and at the same time keeping the object safe.

The results obtained from Experiment 3 highlighted that the gripper can successfully complete grasping and transportation tasks with different objects, with a success rate in the transportation phase (U-D Test, L-R Test) of ≈ 99%, and an overall success rate of 80%. The best performance was obtained with large spherical objects (ID: 4, 6, 7) which never fell during the experiments. Most of the failures were observed in the grasping phase with small objects (ID: 2, 3) and in the release phase, especially with elongated and box-shaped objects (ID: 9, 10, 13, 14, 15). Grasp

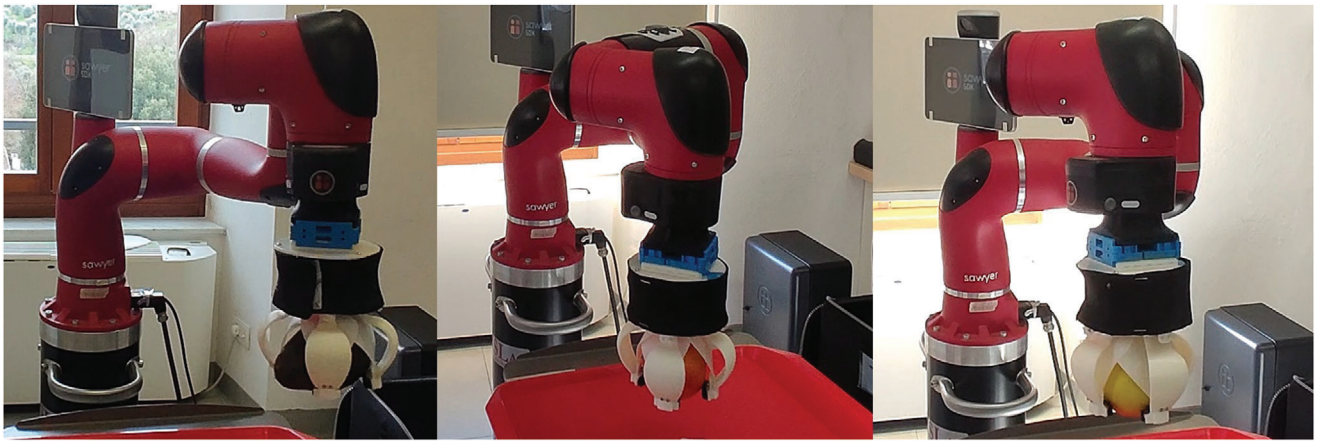


**Figure 10.** Results of Experiment 3: examples of successful grasps of an avocado, an apple and a lemon (YCB).

**Table 5.** Results of Experiment 4: success rate at different transportation velocities.

| ID | Object | $v_{35\%}$ | $v_{40\%}$ | $v_{45\%}$ | $v_{50\%}$ |
|---|---|---|---|---|---|
| 12 | Potato | 3/3 | 3/3 | 3/3 | 3/3 |
| 15 | Crackers | 3/3 | 3/3 | 3/3 | 3/3 |

failures were mainly due to the fact that the fingertips close at a fixed distance from one another and, unless the gripper is perfectly aligned with the object, it can happen that not all of them enter in contact with the object if it is small. Issues in the releasing phase were mainly due to the fact that, if the object is not approached correctly by the robot arm, long objects can easily become stuck in the gripper when enveloped. Moreover, the soft petals that were tested cannot fully wrap around elongated objects as they do with spherical ones. In this case, the soft petals act mainly as a cushion, trapping the object with their lateral sides and sometimes they prevent its release. To solve this issue, a different design/shape of the interchangeable soft petals should be adopted. During the transportation phase a single failure was observed for the Banana (YCB), which slipped out of the gripper during the L-R motion. In all other cases, once the grasp was achieved, the gripper passed the tests successfully. The same caging of the object happened in Experiment 4, where no failures were observed during the motion of the robot, even at higher velocities than in Experiment 3.

## 6. Conclusion

In this paper, we presented the design of a soft-rigid gripper that can be considered as a possible solution for handling perishable foods without damaging or bruising them. The main feature of the proposed solution is a soft-rigid actuated palm that envelops and holds grasped objects as if they were in a sort of soft pocket supported by rigid parts. The gripper satisfies also other important requirements including low power consumption and the possibility of detaching and washing the parts that are in contact with the objects.

Despite having a predefined mechanical structure, the proposed design is scalable and can be easily adapted to grasp sets of objects with different sizes. To achieve this, it is worth highlighting that one of the distinctive features of the gripper is its versatility in designing the soft petals. In fact, it is possible to modify their initial shape, to adjust the number of soft petals, and even select different materials for their realization, allowing you to choose the level of friction needed. Moreover, the methodology adopted for gripper design can be applied to develop gripper structures with different shapes, for different and even more specific tasks. The design proposed in this paper allows to grasp, hold, and transport a quite wide range of objects, but it could be further specialized for specific types of objects and specific tasks, e.g. grasping of deformable objects and garbage sorting. However, one limitation of the developed prototype is that when printed in its current configuration, the device is constrained to handle objects of a specific size range, limiting its versatility. Additionally, there is a lack of fine control over torque, which could affect precision during operation, and the material used for the soft leaves could potentially be made softer to minimize its impact on the motor's torque, improving overall performance and efficiency.

Future works will focus on studying other materials and designs for the soft petals, not only considering the grasp performance but also adopting manufacturing techniques that allow to have a smoother surface making the petals easier to cleanse. Furthermore, future investigations will concern the development of 3D-printed petals using conductive and strain-sensing TPU material.[41,42] In this way, it would be possible to detect whether the soft petals are in contact with the object and estimate the average pressure exerted on it. Eventually, the soft petal optimization procedure will be further investigated, considering other criteria, including the capability of enveloping objects with dimensions in a certain range and the damping properties to prevent shocks.

## Supporting Information

Supporting Information is available from the Wiley Online Library or from the author.

## Acknowledgements

This work was supported by the European Union by the Next Generation EU project ECS17 THE - Tuscany Health Ecosystem (PNRR MUR M4 C2 Inv. 1.5, CUP B63C22000680007, Spoke 9: Robotics and Automation for Health).

Open access publishing facilitated by Universita degli Studi di Siena, as part of the Wiley - CRUI-CARE agreement.

## Conflict of Interest

The authors declare no conflict of interest.

## Data Availability Statement

Data sharing is not applicable to this article as no new data were created or analyzed in this study.

## Keywords

grippers and other end-effectors, materials for soft robotics, soft materials and design, soft robot application, safe food handling

Received: September 24, 2024
Revised: November 22, 2024
Published online:

[1] F. Bader, S. Rahimifard, in *Proceedings of the 2nd International Symposium on Computer Science and Intelligent Control*, **2018**, pp. 1–8.
[2] H. Zhou, X. Wang, W. Au, H. Kang, C. Chen, *Precision Agriculture* **2022**, *23*, 1856.
[3] T. Bhattacharjee, M. E. Cabrera, A. Caspi, M. Cakmak, S. S. Srinivasa, in *Proceedings of the 21st International ACM SIGACCESS Conference on Computers and Accessibility* **2019**, pp. 482–494.
[4] Z. Wang, S. Hirai, S. Kawamura, *Front. Robot. AI* **2022**, *8*, 433.

[5] J. F. Elfferich, D. Dodou, C. Della Santina, *IEEE Access* **2022**, *10*, 75428.
[6] A. Billard, D. Kragic, *Science* **2019**, *364*, eaat8414.
[7] J. Zhu, A. Cherubini, C. Dune, D. Navarro-Alarcon, F. Alambeigi, D. Berenson, F. Ficuciello, K. Harada, J. Kober, X. Li, J. Pan, W. Yuan, M. Gienger, *IEEE Robotics & Automation Magazine* **2022**, *29*, 67.
[8] L. Massari, C. M. Oddo, E. Sinibaldi, R. Detry, J. Bowkett, K. C. Carpenter, *Front. Neurorobot.* **2019**, *13*, 8.
[9] J. M. Krahn, F. Fabbro, C. Menon, *IEEE/ASME Trans. Mechatron.* **2017**, *22*, 1276.
[10] J. Hughes, S. Li, D. Rus, in *2020 IEEE International Conference on Robotics and Automation (ICRA)*, IEEE, Piscataway, NJ **2020**, pp. 6913–6919.
[11] L. He, Q. Lu, S.-A. Abad, N. Rojas, T. Nanayakkara, *IEEE robot. autom. lett.* **2020**, *5*, 2714.
[12] Z. Wang, K. Or, S. Hirai, *Robot. Auton. Syst.* **2020**, *125*, 103427.
[13] S. Jain, S. Dontu, J. E. M. Teoh, P. V. Y. Alvarado, *Soft Robotics* **2023**, *10*, 527.
[14] Y. Piskarev, A. Devincenti, V. Ramachandran, P.-E. Bourban, M. D. Dickey, J. Shintake, D. Floreano, *Advanced Intelligent Systems* **2023**, *5*, 2200409.
[15] J. Lee, H. So, *Macromol. Rapid Commun.* **2023**, *44*, 2300352.
[16] G. L. Goh, G. D. Goh, V. P. Nguyen, W. Toh, S. Lee, X. Li, B. D. Sunil, J. Y. Lim, Z. Li, A. K. Sinha, W. Y. Yeong, D. Campolo, W. T. Chow, T. Y. Ng, B. S. Han, *Adv. Mater. Technol* **2023**, *8*, 2301426.
[17] G. Salvietti, Z. Iqbal, I. Hussain, D. Prattichizzo, M. Malvezzi, in *2018 IEEE/RSJ International Conference on Intelligent Robots and Systems (IROS)*, IEEE, Piscataway, NJ **2018**, pp. 4576–4581.
[18] J. Shintake, V. Cacucciolo, D. Floreano, H. Shea, *Adv. Mater. Technol* **2018**, *30*, 1707035.
[19] C. Piazza, G. Grioli, M. Catalano, A. Bicchi, *Annual Review of Control, Robotics, and Autonomous Systems* **2019**, *2*, 1.
[20] M. Dragusanu, S. Marullo, M. Malvezzi, G. M. Achilli, M. C. Valigi, D. Prattichizzo, G. Salvietti, *IEEE robot. autom. lett.* **2022**, *7*, 7479.
[21] M. Dragusanu, G. M. Achilli, M. C. Valigi, D. Prattichizzo, M. Malvezzi, G. Salvietti, in *2022 International Conference on Robotics and Automation (ICRA)*, IEEE, Piscataway, NJ **2022**, pp. 6173–6179.
[22] A. S. Morgan, K. Hang, B. Wen, K. Bekris, A. M. Dollar, *IEEE robot. autom. lett.* **2022**, *7*, 4821.
[23] E. Turco, V. Bo, M. Pozzi, A. Rizzo, D. Prattichizzo, *IEEE robot. autom. lett.* **2021**, *6*, 5215.
[24] Z. Zhang, X. Ni, W. Gao, H. Shen, M. Sun, G. Guo, H. Wu, S. Jiang, *Soft Rob.* **2022**, *9*, 657.
[25] W. Wang, *Macromol. Mater. Eng.* **2020**, *305*, 1900568.
[26] E. W. Schaler, D. Ruffatto, P. Glick, V. White, A. Parness, in *2017 IEEE/RSJ International Conference on Intelligent Robots and Systems (IROS)*, **2017**, pp. 1172–1179.
[27] M. Pozzi, M. Malvezzi, D. Prattichizzo, G. Salvietti, *IEEE/ASME Trans. Mechatron.* **2024**, *29*, 902.
[28] R. Deimel, O. Brock, *Int. J. Robotics Research* **2016**, *35*, 161.
[29] G. Salvietti, Z. Iqbal, M. Malvezzi, T. Eslami, D. Prattichizzo, in *Proc. IEEE Int. Conf. on Robotics and Automation*, Montreal, Canada, **2019**, pp. 2758–2764.
[30] C. B. Teeple, G. R. Kim, M. A. Graule, R. J. Wood, in *2021 IEEE International Conference on Robotics and Automation (ICRA)*, IEEE, Piscataway, NJ **2021**, pp. 11790–11796.
[31] Y. Li, Y. Wei, Y. Yang, Y. Chen, *Engineering Research Express* **2019**, *1*, 015008.
[32] Q. Shao, N. Zhang, Z. Shen, G. Gu, in *2020 17th International Conference on Ubiquitous Robots (UR)*, IEEE, Piscataway, NJ **2020**, pp. 36–43.
[33] M. A. Roa, R. Suarez, *Autonomous Robots* **2015**, *38*, 65.
[34] M. Pozzi, M. Malvezzi, D. Prattichizzo, *IEEE robot. autom. lett.* **2016**, *2*, 329.
[35] F. Negrello, W. Friedl, G. Grioli, M. Garabini, O. Brock, A. Bicchi, M. A. Roa, M. G. Catalano, *IEEE robot. autom. lett.* **2020**, *5*, 1780.
[36] W. Ji, Z. Qian, B. Xu, W. Tang, J. Li, D. Zhao, *J. Food Process Eng.* **2017**, *40*, e12589.
[37] B. Zhang, J. Zhou, Y. Meng, N. Zhang, B. Gu, Z. Yan, S. I. Idris, *Biosyst. Eng.* **2018**, *171*, 245.
[38] E. Ermakova, T. Elberdov, M. Rynkovskaya, *Computation* **2022**, *10*, 54.
[39] T. Xu, W. Shen, X. Lin, Y. M. Xie, *Polymers* **2020**, *12*, 3010.
[40] B. Calli, A. Walsman, A. Singh, S. Srinivasa, P. Abbeel, A. M. Dollar, *Robot. Automat. Mag.* **2015**, *22*.
[41] E. Bilotti, R. Zhang, H. Deng, M. Baxendale, T. Peijs, *J. Mater. Chem.* **2010**, *20*, 9449.
[42] J. F. Christ, N. Aliheidari, A. Ameli, P. Pötschke, *Mater. Des.* **2017**, *131*, 394.